Magnetic field aligned orderly arrangement of Fe_3O_4 nanoparticles in CS/PVA/Fe_3O_4 membranes*

Meng Du(杜萌)[1,2], Xing-Zhong Cao(曹兴忠)[2,†], Rui Xia(夏锐)[2], Zhong-Po Zhou(周忠坡)[1,‡], Shuo-Xue Jin(靳硕学)[2], and Bao-Yi Wang(王宝义)[2]

[1] *Henan Key Laboratory of Photovoltaic Materials, College of Physics and Materials Science, Henan Normal University, Xinxiang* 453007, *China*

[2] *Institute of High Energy Physics, Chinese Academy of Sciences, Beijing* 100049, *China*

(Received 27 September 2017; revised manuscript received 15 November 2017; published online 5 January 2018)

The CS/PVA/Fe_3O_4 nanocomposite membranes with chainlike arrangement of Fe_3O_4 nanoparticles are prepared by a magnetic-field-assisted solution casting method. The aim of this work is to investigate the relationship between the microstructure of the magnetic anisotropic CS/PVA/Fe_3O_4 membrane and the evolved macroscopic physicochemical property. With the same doping content, the relative crystallinity of CS/PVA/Fe_3O_4-*M* is lower than that of CS/PVA/Fe_3O_4. The Fourier transform infrared spectroscopy (FT-TR) measurements indicate that there is no chemical bonding between polymer molecule and Fe_3O_4 nanoparticle. The Fe_3O_4 nanoparticles in CS/PVA/Fe_3O_4 and CS/PVA/Fe_3O_4-*M* are wrapped by the chains of CS/PVA, which is also confirmed by scanning electron microscopy (SEM) and x-ray diffraction (XRD) analysis. The saturation magnetization value of CS/PVA/Fe_3O_4-*M* obviously increases compared with that of non-magnetic aligned membrane, meanwhile the transmittance decreases in the UV-visible region. The o-Ps lifetime distribution provides information about the free-volume nanoholes present in the amorphous region. It is suggested that the microstructure of CS/PVA/Fe_3O_4 membrane can be modified in its curing process under a magnetic field, which could affect the magnetic properties and the transmittance of nanocomposite membrane. In brief, a full understanding of the relationship between the microstructure and the macroscopic property of CS/PVA/Fe_3O_4 nanocomposite plays a vital role in exploring and designing the novel multifunctional materials.

Keywords: microstructure, CS/PVA/Fe_3O_4 membrane, positron annihilation, magnetic properties

PACS: 78.70.Bj, 61.05.–a, 81.07.Pr, 82.35.Np **DOI:** 10.1088/1674-1056/27/2/027805

1. Introduction

Polymer matrix nanocomposites, which exhibit distinct physicochemical characteristics by incorporating inorganic fillers into polymer networks, have received much attention due to their various industrial applications in drug delivery, water treatment, food industry, aeronautical and aerospace structures.[1–6] Recently, magnetic responsive polymer composite membranes have attracted tremendous interest in the fields of gas separation, ultrafiltration and biomedical, mainly because of their effective transport structures.[7–11] The Fe_3O_4 serving as effective magnetically sensitive filler has been widely investigated to fabricate polymer–inorganic hybrid materials due to its biocompatibility and chemical stability over physiological circumstances in addition to its natural magnetic response.[12–15] Chitosan (CS) is the most important derivative of chitin, and chitin is the second most important natural polymer in the world.[16] The CS, used in food, cosmetics, biomedical applications, has been widely investigated due to its outstanding biocompatibility, and appropriate biodegradability.[17] The CS-Fe_3O_4 membrane fabricated by combining infiltration and magnetic alignment was found to have a higher flux than the corresponding non-magnetized membrane in pervaporation for ethanol dehydration.[18] The addition of Fe_3O_4 nanoparticles changed the packing of CS molecular chains, increased the free-volume cavities in the interface region and enhanced the permeability of hybrid membranes further. Magnetic aligned Fe_3O_4 nanoparticles-based composite materials with other polymers matrix have been reported in many papers.[14,18–21] Poly vinyl alcohol (PVA) has excellent solvent resistance, membrane-forming ability, biodegradable, biocompatible and nontoxic properties, which makes it a possible candidate material for use in biomedicine.[22] As a kind of biomedical material, PVA/CS is more favorable for the cell culture than the pure PVA, and CS/PVA membrane is a potential candidate material in tissue engineering applications due to the biocompatibility and mechanical properties.[23] The magnetic biodegradable Fe_3O_4/CS/PVA membrane has been considered to be one of the promising biomaterials for bone regeneration.[24] However, most researchers have devoted their efforts to exploring new methods with tuning the distribution of functional fillers or developing new materials to modify properties such

*Project supported by the National Natural Science Foundation of China (Grant Nos. 11475197, 11575205, 11404100, and 11304083) and the Key Scientific and Technological Project of Henan Province, China (Grant No. 102102210186).

†Corresponding author. E-mail: caoxzh@ihep.ac.cn

‡Corresponding author. E-mail: zpzhou@htu.edu.cn

as ultrafiltration, gas separation, magnetic, electrical, optical and mechanical properties,[25,26] only a few research studies concentrate on the role of sub-nanoscopic structure in the evolved properties. Sharma *et al.* investigated the role of the microscopic structure at interphase in a PVA-metal organic framework (MOF) nanocomposite in the evolved thermo–mechanical property.[27] Due to attractive interfacial interaction between the surface of zeolitic imidazolate framework (ZIF) particles and PVA chains, the microscopic structure in the interfacial region is changed, indicating the enhancement in rigidity of nanocomposites. Wang *et al.* further studied the function of microscopic structure transition in the effective carbon capture and in grapheme oxide membrane.[28] These studies have shown that it is essential to understand the complex relation between the microstructure and the macroscopic properties of nanocomposites, as a fundamental step to design novel materials further. Nevertheless, a full understanding of the relation between the microstructure and the evolved magnetic and optical properties of the magnetic anisotropic membranes, is still rarely reported.

Unlike conventional measurement techniques such as x-ray diffraction (XRD), Fourier transform infrared spectroscopy (FT-IR) and field emission scanning electron microscopy (SEM) which can provide nearly almost direct information about the microstructure, the position annihilation spectroscopy (PAS) has been used as a sensitive probe to investigate the microstructures of polymeric matrix nanocomposites, providing the information of molecular level packing about the complex bulk material structure.[29] Position annihilation lifetime spectroscopy (PALS) is one of the most common characterization techniques of PAS, which can provide the information about the free volume microvoid properties of the hybrid materials through their lifetime measurements. Recently, the PALS technique has been widely used as a probe to study the microstructures and the correlated positron annihilation characteristics in the fillers cross-linked polymer systems.[29–32] The induction of filler in the polymer matrix can change the original molecular chain packing and free volume nanohole properties. Generally, after positrons implanting into polymeric materials from a radioactive source, a large number of positrons are converted into positronium (Ps) rather than annihilating with electron directly. When positrons are located in the large holes of polymer matrix or in the interfacial region between polymer and functional fillers, the intrinsic lifetime of o-Ps is 142 ns. When located in the free volume of the polymer material, the positrons will annihilate through double gamma photons by picking up an opposite spin electron from the surrounding medium, which is called pick-off annihilation, shortening its lifetime to a few nanoseconds. In other words, o-Ps are located, formed and annihilated finally in the free volume. The lifetime and intensity of o-Ps represent the size and concentration of free volume in polymer, respectively.

In this paper, the magnetic and non-magnetic aligned CS/PVA/Fe_3O_4 nanocomposite membranes are prepared by a magnetic-field-assisted solution casting method. Through the controlled experiments, we mainly study the microstructure and the macroscopic properties of nanocomposites. The morphology of the membrane is characterized by using SEM. The crystalline structure and the chemical bonding changes of membranes are confirmed by XRD and FT-IR, respectively. To investigate the complex relationship between the microstructure and the optical and magnetic property of nanocomposites, PALS, UV-vis transmittance spectra and vibrating sample magnetometer (VSM) testing are carried out. The PALS offers the information about free volume properties, which is based on sub-nano level molecular packing of hybrid membranes. In addition, the effects of an externally applied magnetic field on optical and magnetic behaviors are also discussed.

2. Experiment

2.1. Materials

Chitosan (CS) (degree of deacetylation = 98% −99%, $M_w = 1.2 \times 10^5$ g/mol, purity 98%) was supplied by Zhejiang Shaoxing Bio-technology. Poly (vinyl alcohol) (PVA) (purity 98%), ethylene glycol (purity 98%) and poly ethylene glycol, 2000 (PEG2000) (average Mn 2000) were purchased from Sinopharm Chemical Reagent Co., Ltd, China. Iron chloride hexahydrate ($FeCl_36H_2O$), sodium acetate anhydrous (NaAc) and glycerol (purity 99%) were purchased from Aladdin Co., Ltd, China. Reagents used in this study were all of analytical grade and directly used without any further purification.

2.2. Sample preparation and characterization

Fe_3O_4 nanoparticles were synthesized in advance by a solvothermal reduction method according to Ref. [33]. The Fe_3O_4 nanoparticles were modified by polyethylene glycol 2000. For preparing CS/PVA/Fe_3O_4 membranes, 2-g CS powders were dissolved in 100-mL acetic acid (2 vol%), and PVA solution (5 g·d·L^{-1}) was obtained by oil bath heating in deionized water at 90 °C for 2 h. Then, these two solutions were mixed at a volume ratio of CS : PVA = 40 : 60 to form homogeneous precursor solution. The Fe_3O_4 nanoparticles were mixed at 0, 0.5, and 1 wt% in the CS/PVA precursor solution (70 mL) by continuously stirring. Then 1-mL glutaraldehyde solution (0.25 wt%) and 1 mL glycerol were added into the resulting CS/PVA precursor solution in sequence. Finally, the mixture was poured into a glass petri dish and dried at 40 °C for 3–4 days. During the fabrication of magnetic membrane, two cuboid permanent magnets N35 (50 mm×25 mm×25 mm) were applied for 2 days. The samples were named CS/PVA/$Fe_3O_4(x)$-$M(y)$ (where x represents

the doped fraction of Fe_3O_4 nanoparticles; M denotes the magnetic field, and y refers to the magnetic induction intensity, $y = 0.4$ T in this paper).

The morphologies of CS/PVA/Fe_3O_4(x)-M(y) membranes were observed by FESEM (Hitachi S-4800). The phase compositions of membranes were determined by XRD (D8 Advance). The FTIR spectra were recorded by using a Thermo Scientific Nicolet IN10MX instrument with a liquid–nitrogen cooled detector in a range from 4000 cm^{-1} to 700 cm^{-1}. The UV-vis transmittance spectra were obtained using a UV-vis spectrophotometer (Cary 5000 UV-vis-NIR, Australia). Magnetic properties were measured using a vibrating sample magnetometer (VSM) with a physical property measurement system (PPMS, Quantum Design).

2.3. Positron annihilation measurements

The as-obtained samples were heated at 40 °C for 5 h–6 h prior to the measurements to ensure the absorbed water from the samples was removed entirely. The positron annihilation measurements were carried out at the room temperature in the air atmosphere by using an EG & G ORTEC fast–slow coincidence system with a time resolution of 210 ps. The positron source (^{22}Na, 13 μCi) was fabricated with carrier-free NaCl deposited between two kapton foils each with a thickness of ~ 7 micrometer. The positron source was sandwiched between two stacks of samples with a size of 1 cm×1 cm to guarantee that all the positrons annihilated within the sample completely. Each positron annihilation lifetime spectroscopy (PALS) contained $\sim 2.0 \times 10^6$ counts. A standard Si crystal was used as reference material to evaluate source correction (fraction of positrons annihilating from source material and kapton foils). All the lifetime spectra were analyzed by using LT-9 routine with three exponential components. The routine MELT was used to fit the PALS spectra to evaluate the continuous distribution function of annihilation rate from lifetime spectra. A semi-empirical equation

$$\tau = [1 - r/(r+\Delta r) + \sin((2\pi r)/(r+\Delta r))/(2\pi)]^{-1}/2 \quad (1)$$

correlates o-Ps annihilation lifetime (τ_3) with the radius of the free volume cavity, r_3 ($\Delta r = 0.1656$ nm).[34–36] The free volume fraction (f_{vol}) of membranes were calculated with the following equation:

$$f_{vol} = \lambda(4\pi r_3^3)I_3/3, \quad (2)$$

where $\lambda = 10$.

3. Results and discussion

Figures 1(a) and 1(b) show SEM images of the surface of pure CS/PVA and as-obtained Fe_3O_4 nanoparticles, respectively. Approximate uniform spherical crystals with an average diameter of about 500 nm are observed. In order to observe the dispersion of Fe_3O_4, the surface and cross-section morphologies of CS/PVA/Fe_3O_4 and CS/PVA/Fe_3O_4-M under the loadings with different numbers of nanoparticles were characterized by SEM. Comparing with CS/PVA/Fe_3O_4 membrane, the surface and cross-section morphology in CS/PVA/Fe_3O_4-M are arranged in chain-like conformation, and thus giving a clear indication of magnetization-induced loading Fe_3O_4 nanoparticles in the CS/PVA matrix.

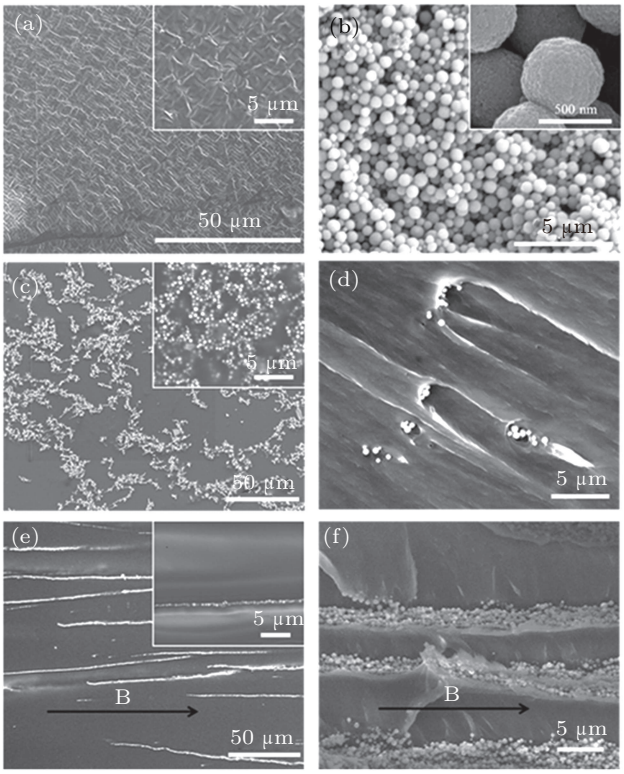

Fig. 1. ((a)–(c) and (e)) Surface and ((d) and (f)) cross section morphologies of (a) pure CS/PVA, (b) pure Fe_3O_4 nanoparticles, ((c) and (d)) CS/PVA/Fe_3O_4, and ((e) and (f)) CS/PVA/Fe_3O_4-M nanocomposite membranes.

The XRD patterns of pure CS/PVA, CS/PVA/Fe_3O_4, and CS/PVA/Fe_3O_4-M are shown in Fig. 2. The characteristic diffraction peak for pure CS/PVA is observed at $2\theta \sim 19.5°$, accompanied with a broad peak at $2\theta \sim 40.6°$.[23,37] On incorporation of Fe_3O_4, it is observed that these peaks become narrower and weaker, indicating the crystallinity of polymer chains decreasing and six new sharp peaks located at $2\theta = 30.0°$, $35.5°$, $43.1°$, $53.4°$, $57.0°$, and $63.0°$, which are in accordance with the inverse cubic spinel structure of Fe_3O_4 (JCPDS19-0629) with the six crystal planes (220), (311), (400), (422), (511), and (440). It is evident that in the case of the presence of an external magnetic field, the relative crystallinity of CS/PVA/Fe_3O_4-M is lower than that of CS/PVA/Fe_3O_4 with the same filler content, and more sharper peaks for Fe_3O_4, indicating stronger aggregations of Fe_3O_4 nanoparticles for the former. The reduced crystallinity in the presence of Fe_3O_4 nanoparticles probably results from the

restricted dynamical motion of the bonded polymer chains, which is defined as molecule movement restriction.

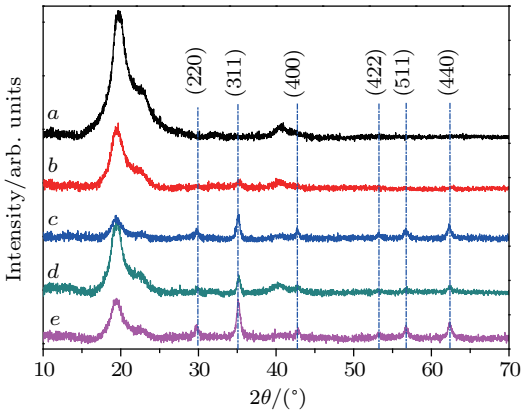

Fig. 2. (color online) XRD patterns of (curve *a*) CS/PVA, (curve *b*) CS/PVA/Fe_3O_4 (0.5 wt%), (curve *c*) CS/PVA/Fe_3O_4 (0.5 wt%)-*M*, (curve *d*) CS/PVA/Fe_3O_4 (1 wt%), and (curve *e*) CS/PVA/Fe_3O_4 (1 wt%)-*M* nanocomposite membranes.

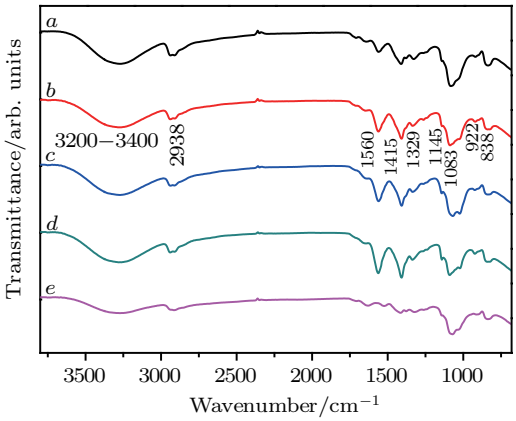

Fig. 3. (color online) Infrared spectra of (curve *a*) CS/PVA, (curve *b*) CS/PVA/Fe_3O_4 (0.5 wt%), (curve *c*) CS/PVA/Fe_3O_4 (0.5 wt%)-*M*, (curve *d*) CS/PVA/Fe_3O_4 (1 wt%), and (curve *e*) CS/PVA/Fe_3O_4 (1 wt%)-*M* nanocomposite membranes.

Figure 3 shows the FTIR spectra of the pure CS/PVA, CS/PVA/Fe_3O_4, and CS/PVA/Fe_3O_4-*M* nanocomposites. The absorption features appearing at 3200 $cm^{-1} \sim 3400$ cm^{-1} observed in both curves are ascribed to the stretching vibration absorption peaks of the –OH and –NH_2.[38,39] The characteristic broad bands around 922 cm^{-1} and 1145 cm^{-1} are assigned to the saccharine structure of CS.[40] The absorption band which appears at 1560 cm^{-1} can be assigned to the –NH_2 blending vibration. The characteristic absorption peaks at 2938, 1415, and 1329 cm^{-1} are attributed to the –CH_2, –CH–OH, and –CH–OH resonance of PVA, respectively.[23,41] The absorption bands at 1083 cm^{-1} and 833 cm^{-1} are attributed to –C–O stretching vibration and –C–C in-plane rocking vibration respectively. On the incorporation of Fe_3O_4 nanoparticles, there is no significant change in the infrared spectra, which indicates that there is no chemical bonding between polymer molecule and Fe_3O_4 nanoparticle.[24,31] The distribution of Fe_3O_4 fillers in the polymer matrix depends mainly on the interaction between polymer molecules and fillers. Because of the flexible CS/PVA polymer chains and the electrostatic interaction between polar groups of the polymer molecules and fillers, the Fe_3O_4 nanoparticles in CS/PVA/Fe_3O_4 and CS/PVA/Fe_3O_4-*M* are wrapped by the chains of CS/PVA, resulting in a relative rearrangement of attached molecules chains along this rigid template.

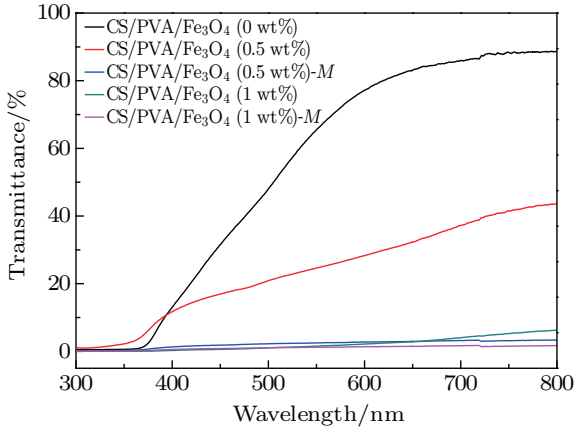

Fig. 4. (color online) The UV-visible transmittance spectra of CS/PVA/$Fe_3O_4(x)$ and CS/PVA/$Fe_3O_4(x)$-*M* ($x = 0$, 0.5, 1 wt%) nanocomposite membranes.

In order to study the effects of external magnetic field inducement on the physical and chemical properties of the nanocomposites, the optical transmittance measurement, subnanoscopic structural measurement of nanocomposites and magnetic testing are carried out. Figure 4 shows the UV-visible transmittance spectra for pure CS/PVA and the nanocomposites membranes. This figure indicates that on the incorporation of Fe_3O_4 fillers, the transmittance of each of the nanocomposite membranes in visible region declines sharply at higher Fe_3O_4 loading. It is observed from 1wt% loading that almost no light transmission appears in the UV region of 300 nm–800 nm due to the increased light scattering caused by agglomerated Fe_3O_4 nanoparticles.[42] In addition, it is clear that the introduction of external field results in magnetization-induced agglomeration of Fe_3O_4 nanoparticles in polymer matrix, and consequently an analogous optical barrier belt is formed, which lowers the transmittance of nanocomposite membrane as confirmed from the significant reduction on the reach of 0.5 wt% loading under magnetic field.

Table 1. The values of o-Ps lifetime τ_3 and free volume fraction f_{vol} of CS/PVA/$Fe_3O_4(x)$ and CS/PVA/$Fe_3O_4(x)$-*M* ($x = 0$, 0.5, 1 wt%) nanocomposites' membranes.

Sample	τ_3/ns	I_3/%	r^3/nm	f_{vol}
CS/PVA/Fe_3O_4 (0 wt%)	1.720	11.4	0.2584	0.0823
CS/PVA/Fe_3O_4 (0.5 wt%)	1.619	12.2	0.2477	0.0776
CS/PVA/Fe_3O_4 (0.5 wt%)-*M*	1.522	9.50	0.2369	0.0529
CS/PVA/Fe_3O_4 (1 wt%)	1.410	13.5	0.2237	0.0633
CS/PVA/Fe_3O_4 (1 wt%)-*M*	1.473	11.4	0.2312	0.0590

To investigate the sub-nanoscopic molecular packing in CS/PVA/Fe_3O_4 hybrid membrane, the free volume properties of CS/PVA and CS/PVA/Fe_3O_4 nanocomposites are characterized using the positron annihilation technique. It is well known that the variations in free volume and hole properties are usually investigated by using an ortho-positronium (o-Ps) probe. Thus PALS spectra of CS/PVA and the nanocomposites are analyzed using LT-9 program and the results are reported in Table 1. The three lifetime components (τ_3) and their corresponding intensity (I_3) are ascribed to o-Ps pick-off annihilation in each of these samples. Meanwhile, the o-Ps lifetime is converted into nanoholes radius (r_3) by using the classical quantum-based formula with a spherical pore geometry. Thus the obtained o-Ps intensity and the average radius are further transformed into the fractional free volume (f_{vol}) using Eq. (2), which provides superior information, rather than just using the o-Ps lifetime and intensity as individual parameters. From Table 1 it is clear that compared with the unfilled CS/PVA membrane, the fractional free volumes of both CS/PVA/Fe_3O_4 and CS/PVA/Fe_3O_4-*M* membranes decrease. The decrease of f_{vol} value is due to the electrostatic interaction between active groups on polymer chains and the functionality available at the nanoparticle surface. Therefore, it is concluded that as a result of the presence of Fe_3O_4 nanoparticles, the original hydrogen bonded structure of semi-crystalline CS/PVA matrix is disrupted, conferring these membranes with more compact chain packing and smaller fractional free volume. According to the conventional theories of positron annihilation in polymer material, the disordered material shows a size and shape distribution of free volume that leads to distribution of o-Ps lifetime around its mean, and the discrete component analysis only presents an average picture of modification in the so-called free volume hole density. Thus the program MELT is used to fit the PALS spectra to evaluate the distribution of positron lifetimes.

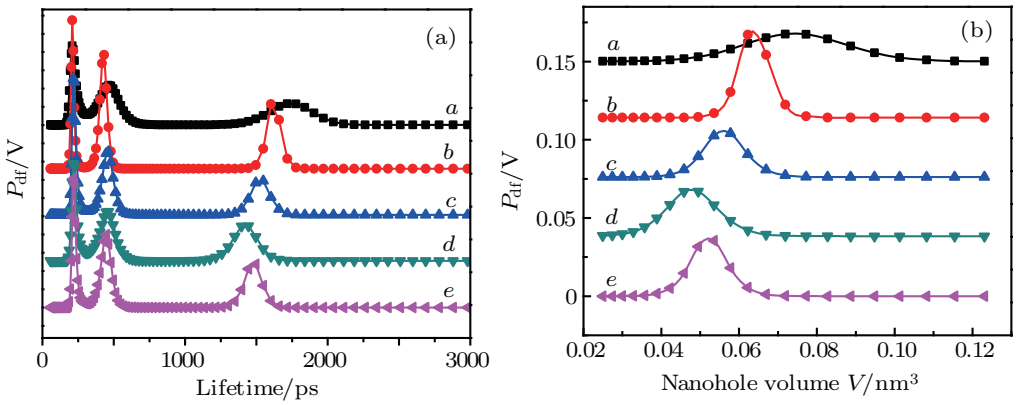

Fig. 5. (color online) (a) Continuous lifetime distribution curves and (b) nanohole volume distributions of (curve *a*) CS/PVA, (curve *b*) CS/PVA/Fe_3O_4 (0.5 wt%), (curve *c*) CS/PVA/Fe_3O_4 (0.5 wt%)-*M*, (curve *d*) CS/PVA/Fe_3O_4 (1 wt%), and (curve *e*) CS/PVA/Fe_3O_4 (1 wt%)-*M* nanocomposite membranes, respectively.

The continuous lifetime distributions of unfilled CS/PVA and CS/PVA-Fe_3O_4 nanocomposites are shown in Fig. 5, indicating that all of the values of o-Ps lifetime or the size distribution of free volume nanoholes decrease with Fe_3O_4 loading, which is in accordance with the result from discrete component analysis. In addition, only one peak is observed in CS/PVA-Fe_3O_4 nanocomposites at longer lifetime component than in pure CS/PVA nanocomposites, indicating the aggregation or poor dispersion of Fe_3O_4 nanoparticles in the matrix. Reports from many similar studies have shown that two peaks are usually observed in the o-Ps lifetime distribution: the second peak is at higher value and the first one at lower value than the corresponding values in the pristine sample, indicating the formation of two regions (local ordered region and amorphous region) with different sizes of nanoholes as a result of polymer-filler interactions. Thus, it is clear that the o-Ps lifetime distribution in the present case provides information about the free-volume nanoholes present in the amorphous region, and as a result of interaction between polymer chains and surface functionalities, the disrupted hydrogen bonded structure of semi-crystalline CS/PVA produces smaller size nanoholes with compact chains packed in the amorphous region.

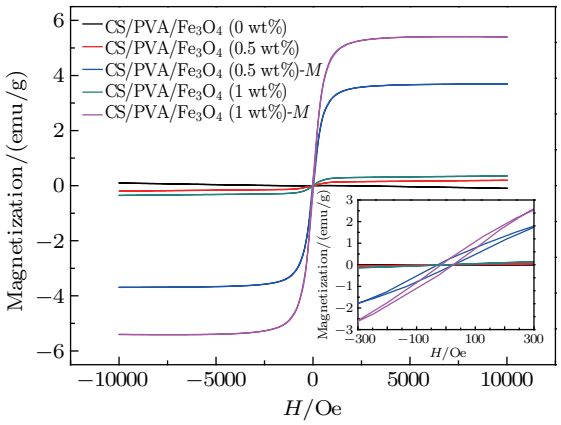

Fig. 6. (color online) Room temperature *M*–*H* hysteresis curves of CS/PVA/Fe_3O_4(x) and CS/PVA/Fe_3O_4(x)-*M* (x = 0, 0.5, 1 wt%) nanocomposite membranes. Inset shows hysteresis at lower fields.

To further evaluate the magnetic properties of the CS/PVA-Fe_3O_4 nanocomposites, VSM measurements are carried out. Figure 6 shows the typical hysteresis loop curves for pure CS/PVA and CS/PVA-Fe_3O_4 nanocomposites having different filler content, indicating their typical ferromagnetic behaviors. On the incorporation of Fe_3O_4, the saturation magnetization (M_s) is changed significantly, and M_s increases from 0.195 emu/g for CS/PVA/Fe_3O_4 (0.5 wt%) to 3.692 emu/g for CS/PVA/Fe_3O_4 (1 wt%). In particular, a significantly increased M_s due to the introduction of external field in film-forming process compared with non-magnetic condition is observed, indicating the presence of enhanced magnetic vector ordering. It is conjectured that most of the magnetic nanoparticles are concentrated on the chain-like conformation due to the magnetic induction effect, thus promoting the inter-particle magnetic dipolar–dipolar interactions.[20,43] With a chain-like structure, the projection of the magnetization vector along the field direction would be higher than that for a random distribution of Fe_3O_4 nanoparticles in the CS/PVA matrix with a large shape anisotropy effect.[43–45] This result indicates that despite being magnetic response to Fe_3O_4 nanoparticles wrapped by polymer chains, the magnetization-induced loading nanoparticles in CS/PVA matrix are much more magnetizable and have the potential applications in manufacturing the nano-particle magnetic nanocomposite films.

4. Conclusions

In this paper, the magnetic ordered CS/PVA/Fe_3O_4 nanocomposite membranes are prepared by a magnetic-field-assisted solution casting process. Due to a co-operative effect between the hydrogen bonding interactions of the CS/PVA matrix and the external field induced magnetic moment interactions, the magnetization-induced loading Fe_3O_4 nanoparticles exhibit chain-like arrangement in the CS/PVA matrix as seen from the surface and cross section morphologies. On the incorporating of Fe_3O_4 nanoparticles, the original hydrogen bonded structure of semi-crystalline CS/PVA matrix is disrupted and no chemical bonding is formed between the polymer molecule and the filler, conferring these membranes with more compact chain packing and smaller fractional free volume, which are confirmed by PALS, XRD, and FTIR data. In addition, it is indicated that the introduction of external field results in forming an analogous optical barrier belt, which lowers the transmittance of nanocomposite membrane in the UV-visible region. Meanwhile, the VSM data indicate that the saturation magnetization value of CS/PVA/Fe_3O_4-*M* is obviously increased, which is mainly due to the enhanced magnetic vector ordering. It is suggested that the CS/PVA/Fe_3O_4 nanocomposite membranes of magnetic ordered chain-like structure promote the magnetic properties and optical properties. This study offers some valuable ideas to investigate the microstructure and macroscopic properties of magnetic responsive polymer nanocomposites, which have a great application prospect in the future.

References

[1] Zhang J, Wang J F, Lin T, Wang C H, Ghorbani K, Fang J and Wang X G 2014 *Chem. Eng. J.* **237** 462
[2] Cai N, Li C, Han C, Luo X G, Shen L, Xue Y N and Yu F Q 2016 *Appl. Surf. Sci.* **369** 492
[3] López-de-Dicastillo C, Jordá M, Catalá R, Gavara R and Hernández-Muñoz P 2011 *J. Agric. Food Chem.* **59** 11026
[4] Popescu R C, Fufă M O M, Grumezescu A M and Holban A M 2017 *Academic Press* **2017** 421
[5] Jalvandi J, White M, Gao Y, Truong Y B, Padhye R and Kyratzis I L 2017 *Mater. Sci. Eng. C* **73** 440
[6] Fulco A P P, Melo J D D, Paskocimas C A, de Medeiros S N, de Araujo Machado F L and Rodrigues A R 2016 *NDT & E Int.* **77** 42
[7] Thévenot J, Oliveira H, Sandre O and Lecommandoux S 2013 *Chem. Soc. Rev.* **42** 7099
[8] Steinert B W and Dean D R 2009 *Polymer* **50** 898
[9] Lin Z Y, Liu Y, Raghavan S, Moon K S, Sitaraman S K and Wong C P 2013 *ACS Appl. Mater. & Interfaces* **5** 7633
[10] Takahashi H, Nagao D, Watanabe K, Ishii H and Konno M 2015 *Langmuir* **31** 5590
[11] Wang Q, Dai J F, Li W X, Wei Z Q and Jiang J L 2008 *Composites Sci. Technol.* **68** 1644
[12] Teja A S and Koh P Y 2009 *Progress in crystal growth and characterization of materials* **55** 22
[13] Ren P G, Wang H, Yan D X, Huang H D, Wang H B, Zhang Z P, Xu L and Li Z M 2017 *Appl. Sci. Manuf.* **97** 1
[14] Huang Z Q, Zheng F, Zhang Z, Xu H T and Zhou K M 2012 *Desalination* **292** 64
[15] Wang H and Zhou S 2016 *Biomater. Sci.* **4** 1062
[16] Rinaudo M 2006 *Prog. Polymer Sci.* **31** 603
[17] Lee K Y and Mooney D J 2001 *Chem. Rev.* **101** 1869
[18] Xing R S, Wu H, Zhao C H, Gomaa H, Zhao J, Pan F S and Jiang Z Y 2016 *Chem. Eng. & Technol.* **39** 969
[19] Brijmohan S B and Shaw M T 2007 *J. Membrane Sci.* **303** 64
[20] Tang Y, Chen Q W and Chen R S 2015 *Appl. Surf. Sci.* **347** 202
[21] Huang Z Q, Chen L, Chen K, Zhang Z and Xu H T 2010 *J. Appl. Polymer Sci.* **117** 1960
[22] Liang J J, Huang Y, Zhang L, Wang Y, Ma Y F, Guo T Y and Chen Y S 2009 *Adv. Funct. Mater.* **19** 2297
[23] Jia Y T, Gong J, Gu X H, Kim H Y, Dong J and Shen X Y 2007 *Carbohydrate Polymers* **67** 403
[24] Yan W, Xue H Z, Yu S, Bing H, Xiao Y H, Xin Z W, Yuan H L and Xu L D 2011 *Biomed. Mater.* **6** 055008
[25] Ashjari M, Mahdavian AR, Ebrahimi NG and Mosleh Y 2010 *J. Inorganic and Organometallic Polymers and Materials* **20** 213
[26] Joshi U A, Sharma S C and Harsha S 2012 *Composites Part B: Eng.* **43** 2063
[27] Sharma S K, Sudarshan K and Pujari P K 2016 *Phys. Chem. Chem. Phys.* **18** 25434
[28] Wang S F, Wu Y Z, Zhang N, He G W, Xin Q P, Wu X Y, Wu H, Cao X Z, Guiver MD and Jiang Z Y 2016 *Energy Environ. Sci.* **9** 3107
[29] Zhao J, Zhu Y W, He G W, Xing R S, Pan F S, Jiang Z Y, Zhang P, Cao X Z and Wang B Y 2016 *ACS Appl. Mater. Interfaces* **8** 2097
[30] Xia R, Cao X Z, Gao M Z, Zhang P, Zeng M F, Wang B Y and Wei L 2017 *Phys. Chem. Chem. Phys.* **19** 3616
[31] Sharma SK, Bahadur J, Patil PN, Maheshwari P, Mukherjee S, Sudarshan K, Mazumder S and Pujari PK 2013 *ChemPhysChem* **14** 1055
[32] Gong Z L, Gong J, Yan X L, Gao S and Wang B 2011 *J. Phys. Chem. C* **115** 18468
[33] Deng H, Li X L, Peng Q, Wang X, Chen J P and Li Y D 2005 *Angewandte Chemie* **18** 2842

[34] Nagel C, Günther-Schade K, Fritsch D, Strunskus T and Faupel F 2002 *Macromolecules* **35** 2071
[35] Eldrup M, Lightbody D and Sherwood J N 1981 *Chem. Phys.* **63** 51
[36] Sharma S K, Prakash J, Sudarshan K, Maheshwari P, Sathiyamoorthy D and Pujari P K 2012 *Phys. Chem. Chem. Phys.: PCCP* **14** 10972
[37] Choo K, Ching Y C, Chuah C H, Julai S and Liou N S 2016 *Materials* **9** 644
[38] Boonsongrit Y, Mueller BW and Mitrevej A 2008 *Eur. J. Pharm. Biopharm.* **69** 388
[39] Vicentini D S, Smania A and Laranjeira M C M 2010 *Mater. Sci. Eng. C-Mater.* **30** 503
[40] Costa-Júnior E S, Barbosa-Stancioli E F, Mansur A A, Vasconcelos W L and Mansur HS 2009 *Carbohydrate Polymers* **76** 472
[41] Zheng H, Du Y M, Yu J H, Huang R H and Zhang L N 2001 *J. Appl. Polymer Sci.* **80** 2558
[42] Zhang Q S, Peng B, Li D, Yang Y and Liu Y L 2014 *IEEE Photon. Technol. Lett.* **26** 2181
[43] Niu H L, Chen Q W, Ning M, Jia Y S and Wang X J 2004 *J. Phys. Chem. B* **108** 3996
[44] Wang J, Chen Q, Zeng C and Hou B 2004 *Adv. Mater.* **16** 137
[45] Wang J, Wu Y J and Zhu Y J 2007 *Mater. Chem. Phys.* **106** 1